sciendo

DOI 10.2478/ama-2019-0029

acta mechanica et automatica, vol.13 no.4 (2019)

MAGNETORHEOLOGICAL FLUIDS BEHAVIOUR IN OSCILLATORY COMPRESSION SQUEEZE: EXPERIMENTAL TESTING AND ANALYSIS

Wojciech HORAK*, Marcin SZCZĘCH*, Bogdan SAPIŃSKI**

*Faculty of Mechanical Engineering and Robotics, Department of Machine Design and Technology, AGH University of Science and Technology, al. Mickiewicza 30, 30-059 Cracow, Poland

** Faculty of Mechanical Engineering and Robotics, Department of Process Control, AGH University of Science and Technology, al. Mickiewicza 30, 30-059 Cracow, Poland

horak@agh.edu.pl, szczech@agh.edu.pl, deep@agh.edu.pl

received 2 October 2019, revised 6 November 2019, accepted 5 December 2019

Abstract: This article deals with experimental testing of magnetorheological fluid (MRF) behaviour in the oscillatory squeeze mode. The authors investigate and analyse the influence of excitation frequency and magnetic field density level on axial force in MRFs that differ in particle volume fraction. The results show that, under certain conditions, the phenomenon of self-sealing can occur as a result of the magnetic field gradient and a vacuum in the working gap of the system.

Key words: magnetorheological fluid, oscillatory compression, magnetic field, squeeze force

1. INTRODUCTION

Magnetorheological fluids (MRFs) are non-uniform suspensions of microsized ferromagnetic particles in the carrier fluid. In engineering applications, hydrocarbon or silicon oil bases are primarily used as carrier fluids. Owing to the magnetic properties of these materials, it is possible to control their rheological parameters by interacting with an external magnetic field. MRFs are used in applications with controlled characteristics, such as vibration dampers, brakes and clutches (Chengye et al., 2011; Farjoud et al., 2008; Guldbakke and Hesselbach, 2006; Kubík et al., 2017). Depending on the type of device, four basic modes of MRF operation can be distinguished: shear mode and valve mode, the essence of which is shear excitation; gradient pinch mode (Goncalves and Carlson, 2009), which is similar to valve flow but at a highly non-uniform magnetic field; and compression mode, in which a complex state of deformation occurs. The compression mode is characterised by the possibility of obtaining significant forces at very small displacements (at a maximum of about a few millimetres). Stresses obtained in MRF when squeezed may approach up to 200 kPa (Tao, 2011). This feature can be advantageous for the development of new MR (magnetorheological) devices, especially dampers (Liu et al., 2019), mounts (Farjoud et al., 2011; Gołdasz and Sapiński, 2011) and bearings (Guldbakke and Hesselbach, 2006), for which the ability to generate large forces and to provide a wide variability range of the performance parameters are of particular importance. Analysis of the MRF squeeze working condition is a complex issue. This is primarily due to the large number of factors affecting the process, that is, squeeze-strengthening effect (Liu et al., 2019; Wang et al., 2019), clumping effect or aggregation of MRF particles (Farjoud et al., 2008; Farjoud et al., 2011), complex deformation state (Horak, 2018; Laun et al., 2008), displaced carrier fluid from the squeeze zone (Laun et al., 2008; Szczęch and Horak., 2017), pressure generated in the MRF under the action of the applied magnetic field (Guo et al.,2012; Horak, 2018), the cavitation effects (Kuzhir et al., 2008) and the complex force progression during the compression process (Guo et al.,2013; Gstöttenbauer et al., 2008; Horak, 2018).

The present article summarises the experimental results and analysis of three MRFs differing in composition, operated in the oscillatory squeeze mode with a constant volume. The purpose of the experiments was to determine the behaviour of MRFs at variable excitation frequencies and magnetic field density. Attention has been paid to the influence of spatial magnetic field distribution on the variability of the value as well as the direction of the squeeze force.

2. CHARACTERISATION OF INVESTIGATED MAGNETORHEOLOGICAL FLUIDS

In this article, we present the results of laboratory tests on the behaviour of selected MRFs operating in the oscillatory compression mode with a constant sample volume.

Tab. 1. Properties of tested MRFs

	Unit	MRF-18	MRF-22	MRF-27
Magnetic particle (by volume)	(%)	18.3	22	27.5
Dynamic viscosity (T_v = 25ºC, B = 0T,γ = 100 s^{-1})	(mPa·s)	80.1	130	276
Density	(g/cm^{-3})	2.137	2.312	2.702
Saturation magnetisation	(kA/m)	~220	~270	~360

Three fluids produced based on oil (hydrocarbon), differing in the content of ferromagnetic particles, were investigated. The MRF-22 is a commercially available fluid marked MRF-122 by Lord Co.; the other two fluids have been obtained by adding or subtracting the base oil to specific samples. Selected physical properties of these fluids are presented in Table 1, and the magnetisation curves are shown in Figure 1. The names of the examined fluids express the volumetric percentage of magnetic particles.

Increasing the amount of ferromagnetic particles in the MRF primarily results in increased magnetisation of saturation. Between MRF-18 and MRF-22, there is a 23% difference in magnetic saturation, and between MRF-18 and MRF-27, the difference is 64%. In addition, the examined fluids differ significantly in their zero-field viscosity. Between MRF-18 and MRF-27, there is a nearly 3.5-fold difference in this parameter.

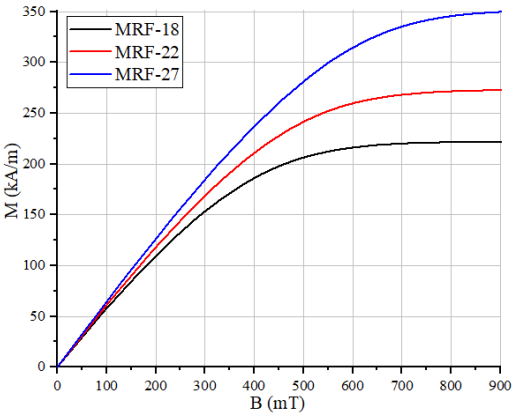

Fig. 1. Magnetisation versus magnetic field density of tested MRFs

In the magnetic field density up to the range of approximately B = 400 mT, all the tested MRFs have an approximate linear M = f(B) characteristic. It can also be noted that in the analysed range of magnetic field density (B < 670 mT), only MRF-18 and MRF-22 should reach the saturation state.

3. EXPERIMENTS

Experiments were conducted in the specially designed experimental setup (Fig. 2a) consisting of a frame (1) supporting a linear servomotor (7), allowing the main position of the measuring system to be changed.

The oscillatory movement of the upper plate (4) is generated by a connecting rod (8) mounted on a cranked shaft (9), driven by a rotary servomotor (11) with timing belt transmission (10). The range of the oscillating plate movement is determined by the crank value 'e'. The force sensor (6) used for measuring the tensile and compression forces is attached to the shaft supported by two linear bearings (5). The position of the movable plate is measured by a non-contact laser sensor (3).

The MRF sample is placed inside the test cell (2) (Fig. 2b) directly above an electromagnet core (17) between a movable plate made of a paramagnetic material (4). The stationary plate (14) is made of a paramagnetic material and reduces ejection of the MRF from the gap. The magnetic circuit is closed by the cell housing (13, 15). The magnetic flux density in the measuring gap is altered by the current in the electromagnet coil (16). In the electromagnet core and in the cell housing, ducts for the coolant were made. This ensures the temperature stabilisation of the system. All experiments were conducted at the constant temperature of 25°C. The diameter of the movable plate d_p was 50 mm, whereas the diameter of the electromagnet core d_c was 45 mm (see Fig. 2c), initial gap height h was 2 mm and the range of motion of the movable plate Δh was 1 mm (compression rate, ε = 0.5).

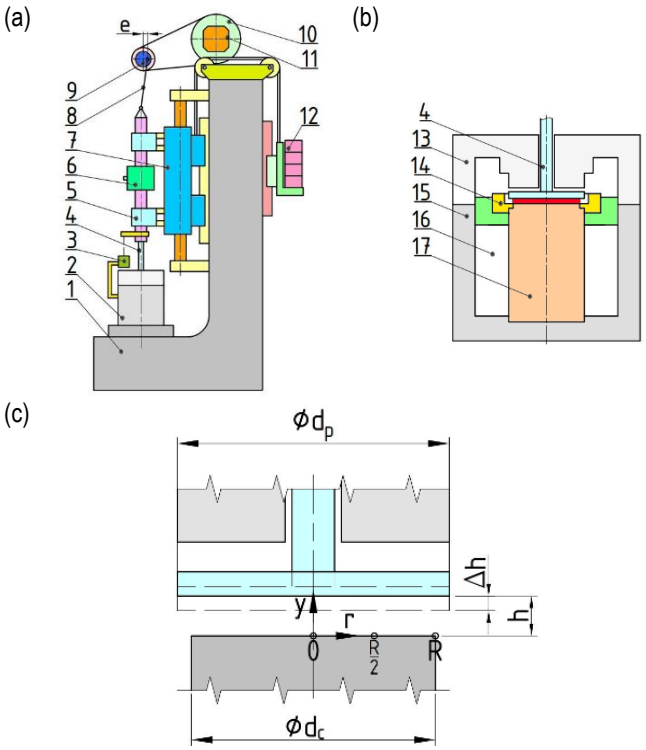

Fig. 2. Schematic diagram: (a) experimental setup, (b) test cell and (c) test geometry

3.1. Scenario

The distribution of the magnetic field density in the working gap was measured by using a teslameter at three points on the diameter of the electromagnet core front face for r = 0, R/2 and R (see Fig. 2c); the measurement results are presented in Figure 3a.

Near the symmetry axis of the system, lower magnetic field density occurs than at the edge of the analysed geometry. For a more detailed investigation of magnetic field spatial distribution, a numerical simulation was carried out by using the finite element method. Figure 3b compares the measurement and numerical simulation results (I = 2 A, dashed line marked in Fig. 3a). A good convergence of simulation to measurement was obtained, with the results presented in Figure 3a also consistent with the analyses presented in Figure 3b. More detailed information about the magnetic field spatial distribution is presented in Szczęch and Horak (2017). The curves of magnetic field density versus current measured at three points are shown in Figure 3b. Owing to the occurrence of the magnetic field density gradient, it should be expected that the higher B values near the edge of the electromagnet core may result in the self-sealing effect of the system (Szczęch and Horak, 2017).

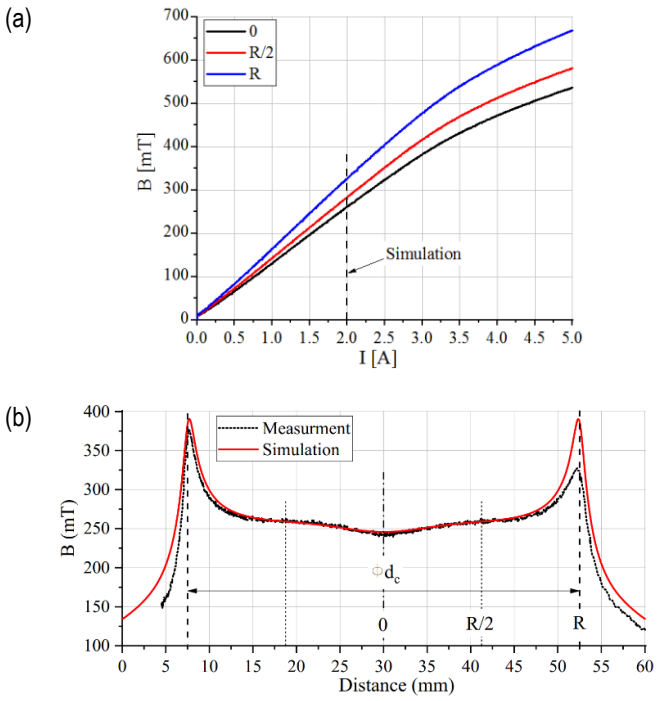

Fig. 3. (a) Magnetic field density versus current measured at three points of the electromagnet core face and (b) distribution of the magnetic field density across the bottom measuring plate

The study was based on measuring the force exerted by the MRF on an oscillatory moving plate during the increase in the magnetic flux density in the range of B = 0 to 670 mT (corresponding to the power supply current of the electromagnet I = 0–5 A). A linear ramp of the current was set for 180 s. Each experiment has been carried out at five extortion frequencies f = 0.1, 0.5, 1, 2 and 3 Hz. Tests were performed for a constant MRF volume, V = 1 mL, which corresponds to the filling rate of the working gap 63% (calculated in relation to h_{min} = 1 mm).

4. RESULTS AND DISCUSSION

The study concerns a comparative analysis of MRFs behaviour. The aim of the study was to determine the range of force variation observed when MRFs are subjected to extortion by oscillatory compression. An example of the measurement result with a determined upper and lower force envelope is shown in Figure 4. The negative sign of the forces indicates that the MRF is in the compression phase, and the positive sign of force refers to the case when the MRF resists the moving plate upwards.

The graphs of maximum compression forces (lower envelopes) of the tested MRFs are presented in Figure 5. For all the tested fluids up to approximately I = 1 A (i.e. B = 150 mT), no significant influence of the composition of samples or the oscillation frequency on the value of the compression force is observed. For higher electromagnet current values, higher forces are obtained for fluids with a higher particle content. The lowest values of compression force are observed for MRF-18 (up to about 365 N) for fluids with higher magnetisation values (MRF-22 and MRF-27) 450 N and 605 N, respectively. A directly proportional relationship between the value of magnetisation of the fluid magnetisation saturation and the observed maximum compression force is visible.

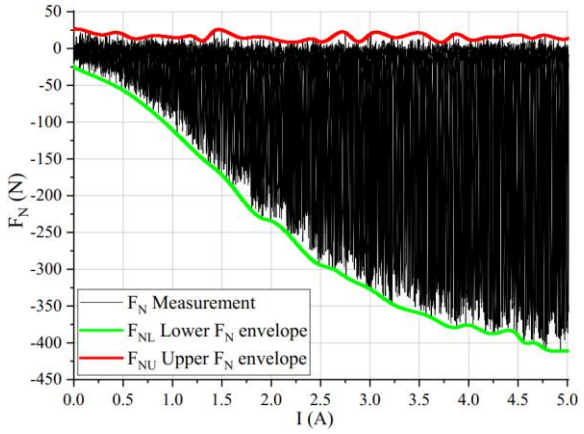

Fig. 4. Sample measurement result with marked upper and lower envelopes (MRF-22, f = 1 Hz)

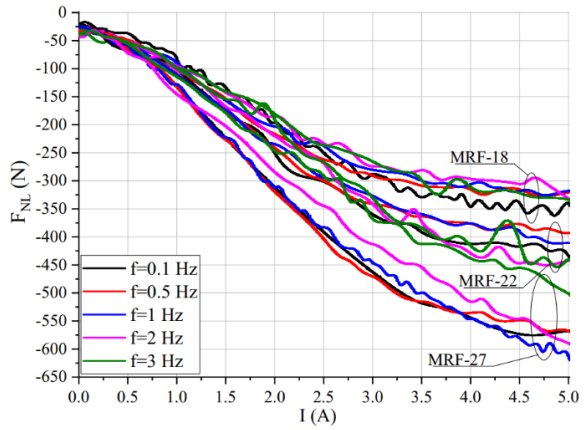

Fig. 5. Lower measured force envelopes F_{NL} versus current I

The graphs of maximum 'tensile' forces (upper envelopes) of the tested MR liquids are shown in Figure 6. For all the tested liquids for I < 1.5 A (B < 250 mT), no significant influence of the frequency and composition of the tested fluids on the measured force is observed. Negative sign force values are observed at the lowest oscillation frequency (f = 0.1 Hz) and for I > 2.5 A (B > 400 mT), indicating that, in this case, the MRF 'pushes' the movable measuring plate out also during the return motion. This may be related to the magnetostatic pressure (Horak et al., 2017; Liu et al., 2019; Mazlan, 2007), which may be related to the influence of columnar structures of magnetic particles on the measuring plate in this case. In the case of the MRF-18 and MRF-22 samples, no significant differences in the measured force were observed (approximately F_{NLmax} = −17 N), whereas for fluids with the highest number of particles, double force (F_{NLmax} = −34 N) was obtained.

In each of the analysed cases, the increase in frequency to 0.5 and 1 Hz resulted in stabilisation of the measured force. Under these test conditions, there is no significant effect of a change in the magnetic field strength on the measured force. The observed positive values of the force (about 20 N) result from the inertia of the measuring system. Preliminary tests carried out without MRF showed the occurrence of forces of up to approximately 15 N.

In the case of force frequency f = 2 and 3 Hz and the current intensity I >2.5 A (B > 400 mT), significant force values with a positive return can be observed. The value of the force increases as the oscillation frequency increases. This phenomenon is visible in all tested fluids. The occurrence of this may be associated with

DOI 10.2478/ama-2019-0029

a vacuum inside the working gap of the measuring system.

The maximum force was observed for MRF-22, F_{NUmax} = 94 N, which indicates the pressure of about p = 60 Pa. This effect can be compared to that which occurs in magnetic fluid seals. The presence of a magnetic field gradient on the edge of the core (see Fig. 3c) may result in the formation of a tight barrier from the MRF between the surface of the electromagnet core and the surface of the moving plate. It should be noted that the values of positive forces are so large that they should be considered when developing devices working in the discussed working conditions.

In Figure 7, graphs of measured force values of (FN) as a function of displacement of a moving plate (Δh) are presented. In the case of f = 0.1 Hz, relatively high values of the compression force can be observed for the initial position of the movable plate (Δh = 0 mm). In this case, the maximum force value was around F_N = −100 N. Similarly, for f = 0.5 Hz, this force is noticeable and is around F_N = −50 N. This behaviour can be explained by the influence of the internal structure of the MRF on the measuring plate. With an increase in the oscillation frequency, the value of this force decreases.

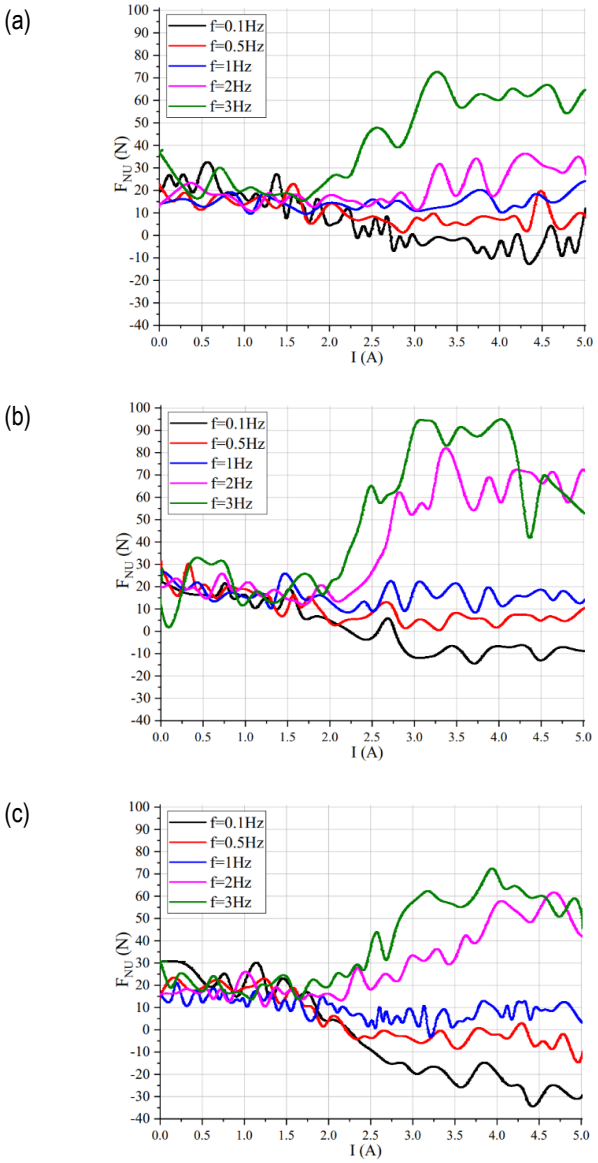

Fig. 6. Upper measured force envelopes F_{NU} versus current I, (a) MRF-18, (b) MRF-22 and (c) MRF-27

For f ≥ 1 Hz, the force in the initial compression phase does not change as the frequency increases. In addition, there are no noticeable differences in the measured compression force for individual MRFs with a low compression rate (ε). In Figure 7d and e, areas of positive force values are visible. It can be noticed that the area of its occurrence covers the range of movement of the plate from Δh = 0.95 to 0.7 mm. Therefore, the vacuum occurs only in the case of a significant degree of compression of the tested fluids (0.95 at the beginning and 0.7 at the end).

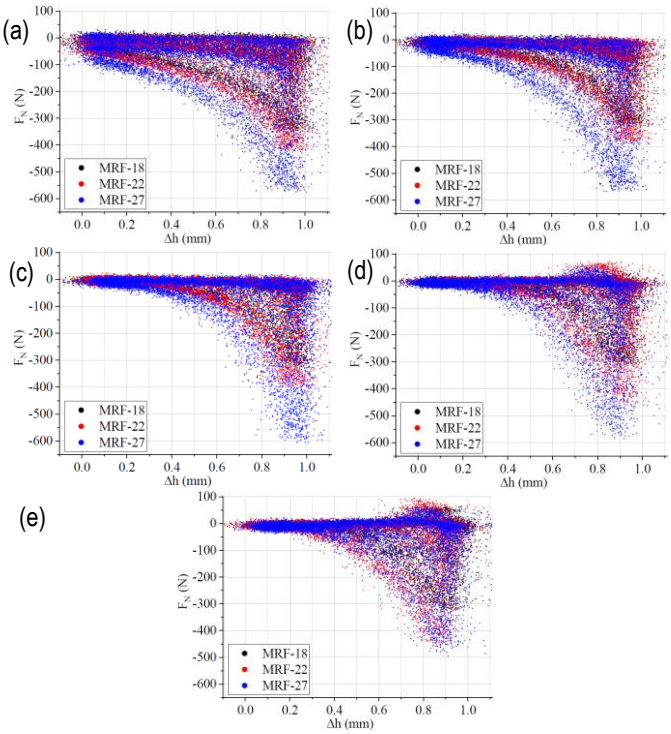

Fig. 7. Measured force F_N versus Δh, (a) f = 0.1 Hz, (b) f = 0.5 Hz, (c) f = 1 Hz, (d) f = 2 Hz and (e) f = 3 Hz

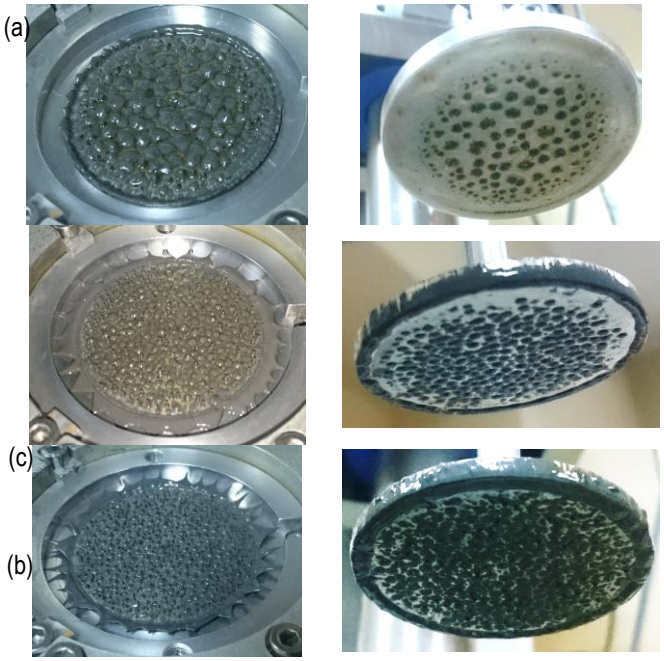

Fig. 8. Photographs of the MRFs after the test; (a) MRF-18, (b) MRF-22 and (c) MRF-27

The photographs also show a change in the structure of the tested fluids, depending on their composition. For the fluid with the lowest content of particles (MRF-18, Fig. 8a), the base fluid precipitations are clearly visible. The concentrations of the MRF are smaller and more dispersed with higher content of magnetic particles (cf. Fig. 8a, b and c).

5. CONCLUSIONS

The results of the experiments and their analysis lead us to the following conclusions:

- The maximum compressive force is obtained for the greatest displacement and is related to the number of magnetic particles and, thus, to the magnetisation curve of the MRF. The volumetric percentage of particles in the carrier fluid can be used as an indicator to estimate the ability of MRF to produce normal compression force.
- The increase in the compression force as a function of displacement is similar to an exponential shape, with the increase in the compression frequency causing the rate of increase to be lower in the range Δh = 0 to 0.3 mm, probably because of the ability to change the internal structure of the particles in the MRF as a result of the deformation. It should be noted that the lower frequency favours the creation of structures.
- Static force is visible in the low enforcement frequency range (up to 0.5 Hz). This process is described in detail in Horak et al. (2017) and Horak (2018).
- In the analysed case, the increase in the compression frequency and magnetisation of saturation encourages the movement of fluids outside the working gap (Fig. 8). This effect was observed only at the frequency of 3 Hz, and the loss of the liquid constituted about 8% of the applied volume.
- Significant 'tensile' forces on the MRF can be generated in the analysed system. This phenomenon may be related to the phenomenon of self-sealing of the measurement gap because of the magnetic field gradient. The result is a vacuum in the working gap of the system. This phenomenon is visible only at higher frequencies of oscillations, that is, from 2 Hz. In addition, positive forces occur only in the case of a significant degree of MRF compression (Δh = 0.95–0.7 mm).

REFERENCES

1. **Chengye L., Fengyan Y., Kejun J.** (2011), Design and finite element analysis of magnetic circuit for disk MRF brake, *Advanced Materials Research*, 181-182, 22–527.
2. **Farjoud A., Vahdati N., Fah Y.** (2008), MR-fluid yield surface determination in disc-type MR rotary brakes, S*mart Materials and Structures*, 17(3), 1–8.
3. **Farjoud A., Craft M., Burke W., Ahmadian M.** (2011), Experimental investigation of MR squeeze mounts, *Journal of Intelligent Material Systems and Structures*, 22, 1645–1652.
4. **Guo C, Gong X, Xuan S, Zong L and Peng C**. (2012), Normal forces of magnetorheological fluids under oscillatory shear, *J. Magn. Magn. Mater*, 324, 1218.
   Guo C., Gong X., Xuan S., Yan Q. and Ruan X. (2013), Squeeze Squeeze behavior of magnetorheological fluids under constant volume and uniform magnetic field, *Smart Materials and Structures*, 22(4), 045020.
6. **Gstöttenbauer N., Kainz A, Manhartsgruber B.** (2008), Experimental and numerical studies of squeeze mode behaviour of magnetic fluid, Proc. IMechE Part C, *J. Mechanical Engineering Science*, 222(12), 2395-2407
7. **Guldbakke J. M., Hesselbach, J.** (2006), Development of bearings and a damper based on magnetically controllable fluids, *J. Phys*., *Condens. Matter*, 18(38), 2959–2972.
8. **Gołdasz J., Sapiński B.** (2011), Model of a squeeze mode magnetorheological mount, *Solid State Phenomena*, 177, 116–124.
9. **Goncalves F.D., Carlson J.D.** (2009) An alternate operation mode for MR fluids – magnetic gradient pinch, *Journal of Physics*, Conference Series, 149(1), 012050.
10. **Horak W. Sapiński B., Szczęch M.** (2017), Analysis of force in MR fluids during oscillatory compression squeeze, *Acta Mechanica et Automatica*, 11 (1), 64–68.
11. **Horak W.** (2018) Modeling of magnetorheological fluid in quasi-static squeeze flow mod, *Smart Materials and Structures*, 27 (6), 065022.
12. **Kubík M., Macháček O., Strecker Z., Roupec, J, Mazůrek I.** (2017), Design and testing of magnetorheological valve with fast force response time and great dynamic force range, *Smart Material and Structures*, 26(4), 047002.
13. **Kuzhir P., López-López M. T., Vertelov G., Pradille C., Bossis G.** (2008), Oscillatory squeeze flow of suspensions of magnetic polymerized chains, *J. Phys.*, Condens. Matter, 20204132.
14. **Laun H.M., Gabriel C., Schmidt G**. (2008), Primary and secondary normal stress differences of a magnetorheological fluid (MRF) up to magnetic flux densities of 1 T, *Journal of Non-Newtonian Fluid Mechanic*, 148(1), 47-56.
15. **Liu W., Luo Y., Yang B., Lu W**. (2019), Design and Mechanical Model Analysis of Magnetorheological Fluid Damper, *American Journal of Mechanics and Applications*, 4(1), 15-19.
16. **Mazlan S.** (2007), The performance of magnetorheological fluid in squeeze mode, *Smart Materials and Structures*, 16(5), 1678-1682.
17. **Szczęch M., Horak W.** (2018), Analysis of the magnetic field distribution in the parallel plate rheometer measuring system, Tribologia, 49(2),117-122.
18. **Tao R.** (2011), Super-strong magnetorheological fluids, *Journal of Physics: Condensed Matter*, 13(50), 979–999.
19. **Wang N., Liu X., Zhang X.,** (2019), Squeeze-Strengthening Effect of Silicone Oil-Based Magnetorheological Fluid with Nanometer Fe_3O_4 Addition in High-Torque Magnetorheological Brake, *Journal of Nanoscience and Nanotechnology*, 1, 19(5), 2633-2639.
20. **Zhang X. J., Farjud A., Ahmadian M., Guo K. H., Craft M**. (2011), Dynamic Testing and Modelling of an MR Squeeze Mount, *Journal of Intelligent Material Systems and Structures*, 22, 1717-1728.

This work is supported by AGH University of Science and Technology under research programs No. 16.16.130.942.